

Spin echo decay at low magnetic fields in a nuclear spin bath

Lukasz Cywiński,^{1,2,*} V. V. Dobrovitski,³ and S. Das Sarma²

¹*Institute of Physics, Polish Academy of Sciences,
al. Lotników 32/46, PL 02-668 Warszawa, Poland*

²*Condensed Matter Theory Center, Department of Physics,
University of Maryland, College Park, MD 20742-4111, USA*

³*Ames Laboratory, Iowa State University, Ames, Iowa 50011, USA*

(Dated: November 9, 2018)

We investigate theoretically the spin echo signal of an electron localized in a quantum dot and interacting with a bath of nuclear spins. We consider the regime of very low magnetic fields (corresponding to fields as low as a militesla in realistic GaAs and InGaAs dots). We use both the exact numerical simulations and the analytical theory employing the effective pure dephasing Hamiltonian. The comparison shows that the latter approach describes very well the spin echo decay at magnetic fields larger than the typical Overhauser field, and that the timescale at which this theory works is larger than previously expected. The numerical simulations are also done for very low values of electron spin splitting at which the effective Hamiltonian based theory fails quantitatively. Interestingly, the qualitative difference in the spin echo decay between the cases of a homonuclear and a heteronuclear bath (i.e. bath containing nuclear isotopes having different Zeeman energies), predicted previously using the effective Hamiltonian approach, is still visible at very low fields outside the regime of applicability of the analytical theory. We have found that the spin echo signal for a homonuclear bath oscillates with a frequency corresponding to the Zeeman splitting of the single nuclear isotope present in the bath. The physics behind this feature is similar to that of the electron spin echo envelope modulation (ESEEM). While purely isotropic hyperfine interactions are present in our system, the tilting of the electron precession axis at low fields may explain this result.

I. INTRODUCTION

The problem of the dynamics of an electron spin coupled by a hyperfine (hf) interaction to a bath of nuclear spins has been a focus of much theoretical attention, since the interaction with the nuclear bath is the most limiting decoherence mechanism in spin qubits based on quantum dots made of III-V materials.^{1,2} While at high magnetic fields ($B \gg 0.1$ T in large GaAs dots when spin echo is considered) the dipolar interactions between the nuclear spins are the main source of dynamics leading to decoherence seen in spin echo (SE) experiment,³⁻⁷ at lower fields the electron spin dephases and relaxes due to hf interaction alone. This process has been studied theoretically for free evolution or SE both by analytical methods^{6,8-18} and by exact numerical simulations.^{10,19-23} Here we focus on the theoretical description of SE decay due to hyperfine interaction alone,^{6,11,12,16,17,21} since the SE experiment is currently the most developed measurement of coherence decay in electrically controlled gated GaAs quantum dots,²⁴⁻²⁶ and there has been a recent progress in performing SE measurements on optically controlled electron spins in quantum dots^{27,28} and spins of electrons bound to donors.²⁹

Most of the analytical approaches were concentrated on the “perturbative” regime^{9,13-15,18} of magnetic fields in which the electron Zeeman energy Ω and the total hf energy $\mathcal{A} \equiv \sum_i A_i$ (where the sum is over all the nuclei and A_i are the individual hf couplings) fulfill $\mathcal{A}/\Omega \ll 1$. Only recently it has been proposed^{16,17} that an analytical calculation can be well-controlled under a much weaker condition of $\delta \equiv \mathcal{A}/\Omega\sqrt{N} \ll 1$ (N being the number

of nuclei interacting with the central spin), allowing the calculation of decoherence at much lower B fields (which only have to be larger than the typical Overhauser field due to the nuclei, which is on the order of a few mT in large GaAs dots). In this theory, as in earlier closely related studies,^{6,11,12} an effective pure dephasing Hamiltonian describing hyperfine-mediated interactions between the nuclei is used. For a pure dephasing problem one can formulate a diagrammatic expansion technique for spin decoherence time evolution, and a class of diagrams of leading order in $1/N$ expansion can be resummed,¹⁷ leading to predictions for narrowed state^{30,31} Free Induction Decay (FID), SE decay, and also decoherence under any other dynamical decoupling^{23,32-35} sequence of ideal π pulses driving the qubit.

In this article we present a comparison between the SE decay calculated using the ring diagram theory (RDT) of Refs. 16,17 and exact simulations of a system with $N=20$ nuclei. In this way we set out to clarify the limits of quantitative applicability of the RDT, i.e. the ranges of electron spin splitting and time-scales on which the analytical theory based on effective Hamiltonian accurately describes the SE decay. We also investigate numerically the regime of very low spin splittings, at which the RDT is bound to fail, and we analyze simplified approaches which can be used to model (at least on a certain timescale) the SE signal in this regime.

The exact results confirm that the RDT is quantitatively accurate as long as $\delta \ll 1$, and that the presence of multiple nuclear isotopes (having different Zeeman splittings) is crucial for qualitatively correct description of the SE decay at these low fields. While with $N = 20$

spins used in the exact calculation it is impossible to unequivocally discern whether it is $\delta \ll 1$ or $\mathcal{A}/\Omega \ll 1$ which is controlling the quantitative agreement, our simulations strongly suggest that the qualitative (or even semi-quantitative) predictions of the RDT still hold even at lower B fields. We observe that RDT correctly predicts many qualitative features of the dephasing process even for $\delta \sim 1$, i.e. the RDT results are valid (at least qualitatively, and at least at certain timescale τ_R) beyond the regime $\mathcal{A}/\Omega \ll 1$. The striking qualitative difference in SE decay between a heteronuclear and a homonuclear system is clearly visible for $\delta \approx 1$ (when $\mathcal{A}/\Omega > 1$), and the timescale at which the majority of the decay (say, by half of the initial amplitude) occurs is reproduced by the RDT. This leads us to the conclusion that the smallness of \mathcal{A}/Ω is not necessary for correct analytical description of the spin echo signal.

Another interesting feature of the low- B SE signal in a homonuclear system is the oscillation of this signal with time at a frequency given by nuclear Zeeman splitting. This feature is clearly visible in our results, and it should not be confused with the oscillations appearing in a heteronuclear situation, when the frequencies are given by the *differences* of nuclear Zeeman energies of different isotopes.^{16,17,26}

The paper is organized in the following way. In Sec. II we give a brief outline of the analytical RDT theory and its limitations, and we describe the system of 20 nuclei to which an exact numerical method of evaluation of spin dynamics is applied. In Sec. III we present the results of the calculations, and in Sec. IV we discuss them and compare them with simplified “box wavefunction” model (in which all the hf couplings are the same). In Appendix A we provide an extended discussion of the influence of choice of the hf couplings on the results of the calculations in a system with $N=20$ nuclei.

II. THEORETICAL APPROACH

The Hamiltonian is given by

$$\hat{H} = \Omega \hat{S}^z + \sum_i \omega_{\alpha[i]} \hat{J}_i^z + \sum_i A_i \mathbf{S} \cdot \mathbf{J}_i, \quad (1)$$

where Ω is the electron spin Zeeman splitting, $\omega_{\alpha[i]}$ is the Zeeman energy of the i -th nuclear spin which belongs to nuclear species α , and the last term is the hf interaction. We employ $J=1/2$ nuclear spins in the paper.

A. Overview of the effective-Hamiltonian-based theory of ring diagram resummation

When Ω is large enough one can perform a canonical transformation on the full hf Hamiltonian given in Eq. (1), which removes the electron-nuclear spin flip terms ($\hat{S}^\pm \hat{J}_i^\mp$) in favour of a hierarchy of intra-bath

hf-mediated interactions involving two or more nuclear spins.^{6,15–17,21} It has been argued^{16,17} that as long as $\delta \ll 1$ and when considering the evolution up to a certain time-scale τ_R , one needs to take into account only the lowest-order term in the the expansion of the effective hamiltonian \tilde{H} :

$$\tilde{H}^{(2)} = - \sum_i \frac{A_i^2}{4\Omega} \hat{J}_i^z + \hat{S}^z \sum_i \frac{A_i^2}{4\Omega} + \hat{S}^z \sum_{i \neq j} \frac{A_i A_j}{2\Omega} \hat{J}_i^+ \hat{J}_j^- (2)$$

where the first two terms are renormalizations of the nuclear and electron Zeeman energies, respectively, and the third term is the hf-mediated interaction.

With such an effective *pure dephasing* Hamiltonian (where the only electron spin operator present is \hat{S}^z) the diagonal elements of the reduced density matrix of the central spin (giving the average spin in the z direction) remain constant in time, and the evolution of the off-diagonal element $\rho_{+-}(t)$ can be mapped onto evaluation of the bath-averaged contour-ordered exponent.^{12,16,17,36–38} This formulation of the problem allows one to employ some of the tools of the diagrammatic perturbation theory, most importantly the linked cluster theorem, using which one can write ρ_{+-} as an exponent of the sum of all the connected diagrams contributing to the original expansion.

The third term in Eq. (2) is a long-range interaction coupling *all* the N nuclei within the bulk of the electron’s wavefunction with comparable strength. For such an interaction all the terms in the perturbative expansion of $\rho_{+-}(t)$ can be classified by their $1/N$ dependence. The leading-order terms can then be resummed and the time-dependence of the SE signal can be easily calculated.^{16,17} Let us stress that both the exponential resummation of the original expression for $\rho_{+-}(t)$ and further resummation of a class of linked diagrams are technically feasible because we use an approximate effective pure dephasing Hamiltonian.

The decoherence due to the bath dynamics caused by the dipolar interactions between the nuclear spins (spectral diffusion) can be calculated in a similar way, but only the second order (in dipolar coupling) diagram needs to be retained in the cluster expansion in order to get a controlled description of SE decay,^{5,6,12} and a very good agreement with spin echo measurements of spins of phosphorus donors in Si was obtained.^{5,39,40} Let us also mention that the theoretical prediction^{4–6} of the coherence decay timescale of $\gtrsim 10 \mu\text{s}$ due to the spectral diffusion at high B in GaAs quantum dots was recently confirmed.²⁶ According to the RDT, in GaAs dots at sub-Tesla magnetic field the hf-mediated interactions give the SE decay which is an order of magnitude faster than the decay due to dipolar interactions,^{16,17} and since we are interested in correct description of coherence dynamics on timescale comparable to its characteristic decay time, we neglect the dipolar dynamics altogether in the low- B regime in which our focus is on relatively short times.

For the relevant here case of spin echo we define the decoherence function $W(t) \equiv \rho_{+-}(t)$ (assuming $\rho_{+-}(0) =$

1), with which the expectation values of the transverse components of the central spin are given by $\langle \hat{S}^x(t) \rangle = \frac{1}{2} \text{Re}W(t)$ and $\langle \hat{S}^y(t) \rangle = -\frac{1}{2} \text{Im}W(t)$.

The RDT calculation of decoherence due to two-spin hf-mediated interactions simply involves diagonalization of $N \times N$ matrix at each time step. Such a T -matrix can be easily calculated, as described in details in Ref. 17, and the decoherence function is given then by the following formula involving the eigenvalues $\lambda_l(t)$ of the T -matrix:

$$W(t) = \prod_l^N \frac{1}{\sqrt{1 + \lambda_l^2(t)}}. \quad (3)$$

Let us note that the pair correlation approximation (PCA) from Refs. 6,11,33 can be extended to the heteronuclear case considered here, and it leads to approximating the decoherence function by $W_{\text{PCA}} = \exp(-\frac{1}{2} \sum_l \lambda_l^2)$. This corresponds to taking only the lowest order term in the linked cluster expansion^{12,17} of $W(t)$, while in the RDT we resum all the terms in this expansion which are of the leading order in $1/N$ at every order in the spin-spin coupling.

The key feature of the spin echo sequence in the high-field ($\delta \ll 1$) regime is that the dephasing of the central spin due to \hat{S}^z -conditioned interaction from Eq. (2) with a single nuclear species (i.e. all the nuclei having the same Zeeman splitting) is practically completely undone by the pulse sequence.^{6,21} However, at magnetic field lower than $B_c \approx \sqrt{\Omega/\Delta\omega} \mathcal{A}/\sqrt{N} |g_{\text{eff}}| \mu_B$ (where $\Delta\omega$ is the typical difference of Zeeman splittings between distinct nuclear species and g_{eff} is the effective g-factor of the electron) the hf-mediated processes between nuclei of different species were predicted to completely dominate the SE decay.^{16,17} This prediction has recently been confirmed experimentally in a spin echo experiment in a double dot singlet-triplet qubit,²⁶ in which the B -dependence of the SE decay and the characteristic oscillations of the SE signal with frequencies $\propto \omega_{\alpha\beta} \equiv \omega_\alpha - \omega_\beta$ have been seen. Let us note that with the parameters used in the calculations below the B field regime in which these heteronuclear process dominate the decay corresponds to $\Omega < \Omega_c \approx 100$ in the units defined below.

B. Approximations inherent in the ring diagram calculation

There are higher-order terms in the expansion of the effective Hamiltonian \tilde{H} , which correspond to virtual processes involving more than two S - J spin flips.¹⁷ These terms also involve increasing numbers of nuclear spins, i.e. there are n -spin interactions in $\tilde{H}^{(n)}$, while the RDT can only deal with two-spin interactions. The exact derivation of these terms quickly becomes very complicated, but we do not expect such an expansion to be useful: when the first higher-order interaction in \tilde{H} becomes important, all the higher order terms become equally relevant. However, in order to illustrate the breakdown of

the RDT we will use in the calculations the two-spin \hat{S}^z -independent interaction which appears in $\tilde{H}^{(3)}$, in which the coupling constants are proportional to $\mathcal{A}^3/N^2\Omega^2$.

A more important approximation underlying RDT is the fact that the effective-Hamiltonian approach neglects the transformation of states associated with the canonical transformation (i.e. only the Hamiltonian is transformed). As a result, no decay of S^z component of the central spin can be obtained. This also has consequences for the decay of the transverse spin components at low B fields, where the effective-Hamiltonian based theory does not reproduce the fast ‘‘visibility loss’’ process.^{6,9,21} The latter process, in which the transverse spin component decays by $\sim \delta^2$ on a time-scale of \sqrt{N}/\mathcal{A} can be captured by an exact simulation or by a theory in which at least some effects of state transformation are retained, see e.g. Ref. 6. A more detailed calculation of this process, which is associated with decay of the S^z component of the central spin, is given in Ref. 9, where the Generalized Master Equation method with the full hf Hamiltonian was used.

The transformation of states corresponds to an entanglement of electron spin with the nuclei (each possible initial bath state gets entangled on a short time-scale with the central spin state). Semiclassically it can be envisioned as a slight tilting of the electron quantization axis from the z direction, which happens due to hf interaction with the collective spin of the nuclei. The latter is semiclassically reproduced as a random vector, and the tilting of the central spin’s z -axis is conditioned upon the size and the direction of this vector.

The visibility loss is only one example of effects which are absent in an effective-Hamiltonian approach. There are also other features, which require the treatment based on the full hf Hamiltonian. The analytical approaches of this kind have only been applied to the case of FID decay in a narrowed nuclear state.^{9,13,14,18} At times much longer than N/\mathcal{A} an asymptotic $1/t^2$ coherence decay was obtained,^{13,14,18} which is not reproduced by the RDT calculation.^{16,17} However at high fields ($\mathcal{A}/\Omega < 1$) most of the narrowed FID decay is described by an exponential e^{-t/T_2} obtained both by the RDT (and PCA at very high fields¹¹) and by the Generalized Master Equation (GME) approach using the full Hamiltonian in Ref. 18, and using the effective Hamiltonian in Ref. 15.

It should be stressed that in the full-Hamiltonian theories it was argued that the convergence of the calculation is guaranteed only when \mathcal{A}/Ω is small, which is a much more restrictive requirement than $\delta \ll 1$ required in RDT theory. However, neglecting the higher-order multi-spin interactions in the effective Hamiltonian was argued¹⁷ to be a good approximation for $\delta \ll 1$ *only up to a certain time-scale* τ_R , so that even if the effects of the state transformation were unimportant, the temporal regime of applicability of RDT is certainly limited. On the other hand, the GME theories seem to give a well-controlled result for *all times*, but in a more restricted regime of magnetic fields. Let us also mention that τ_R

might be different for narrowed FID and SE, so that the conclusions on the relation of our results on SE presented here to the results obtained for narrowed FID with other theories should be drawn carefully.

An experimentally relevant question is whether τ_R is larger than the timescale of significant coherence decay. While the estimate of $\tau_R \sim N/\mathcal{A}$ given previously is currently enough for making contact with recent experiments^{24–26} on spin echo in GaAs where it corresponds to about 10 μ s, establishing a more precise bound is of large current theoretical and possibly future experimental interest.

C. Numerical treatment of the full hyperfine Hamiltonian

In order to establish more firmly the regime of applicability of the RDT one should compare its predictions with exact calculations starting from the full hf Hamiltonian from Eq. (1). In this way it is also possible to investigate the regime of very low B fields (corresponding to $\delta > 1$), in which no comprehensive analytical approach has been successful. In the exact numerical simulation the time-dependent Schrödinger equation for the central spin and the bath is solved using the Chebyshev polynomial expansion of the evolution operator.^{20,22}

Although the nuclear spins in GaAs and InAs have $J = 3/2$ or $9/2$, we use $J = 1/2$ in the paper. The main expected effect of such a simplification is slowing down of the decay (larger nuclear spins are more efficient at decohering the central spin). It allows us however to use the maximal number of nuclei $N = 20$ in an exact simulation, diminishing thus the possibility that differences between the numerics and RDT simply come from the failure of $1/N$ expansion of diagrams describing various processes in the nuclear bath.

In a real quantum dot the number of nuclei interacting appreciably with the electron is commonly defined as $N \equiv \mathcal{A}^2 / \sum_i A_i^2$. We identify this quantity with the finite N used in the simulations. This leads to $\delta \equiv \sqrt{\sum_i A_i^2} / \Omega$. Furthermore, we use energy units in which $\sum_i A_i^2 = 1$, so that δ is equal simply to $1/\Omega$ and $\mathcal{A} = \sqrt{N}$ in these dimensionless units. The time is then measured in units of \sqrt{N}/\mathcal{A} , which in real GaAs dot with $N \approx 10^6$ corresponds to about 10 ns (with $J = 1/2$ the T_2^* decay time of inhomogeneously broadened FID^{10,41} is equal to $\sqrt{8}$ in the dimensionless units used in the figures).

Our calculations correspond to the following experimental procedure. Initially the electron spin is assumed to be directed along the \hat{x} axis in the $|+x\rangle$ state. After evolution for time $t/2$ an instantaneous rotation by π about the \hat{x} axis is applied to the central spin. The expectation value of the \hat{S}^x operator at the final time t is then the SE amplitude, plotted in all the figures as a function of the total pulse sequence time t . The general

formula is given by

$$\langle \hat{S}^x(t) \rangle = \left\langle \langle +x | e^{i\hat{H}\tau} \hat{\sigma}_x e^{i\hat{H}\tau} \frac{\hat{\sigma}_x}{2} e^{-i\hat{H}\tau} \hat{\sigma}_x e^{-i\hat{H}\tau} | +x \rangle \right\rangle \quad (4)$$

where $\langle \dots \rangle = \frac{1}{Z} \text{Tr}_J[\dots]$ is the average over an unpolarized nuclear bath (with $Z = 2^N$), and $\tau \equiv t/2$.

The calculations have been performed on a model system of $N = 20$ nuclear spins coupled to the central spin by hf Hamiltonian from Eq. (1). The hf couplings A_i were drawn from a random distribution, with constraint $\sum_{i=1}^N A_i^2 = 1$. We discuss the choice of such a distribution, and also the sensitivity of the results to the specific choice of A_i , in Appendix A. Here we remark that with $N = 20$ the SE signals are very similar one to another for most the choices of the set of A_i , and below we employ the set of A_i corresponding to a rather typical SE signal. In the hetero-nuclear case we have divided the nuclei into 3 species with 10, 6, and 4 members in order to mimic the ratios of concentrations of various isotopes in GaAs (⁷⁵As, ⁶⁹Ga, and ⁷¹Ga, respectively). The Zeeman splittings ω_α of these 3 species were fixed at 0.02526, 0.0354, and 0.045, again mimicking the ratios of nuclear Zeeman energies in GaAs. Note that the ω_α are kept fixed while the electron Zeeman splitting Ω is varied. Although this does not correspond to realistic situation when all the Zeeman energies are proportional to the B field, it allows us to more clearly separate the effects that the electron and nuclear Zeeman energies have on the time dependence of the SE signal. Let us note that while the ratio $\Omega/\omega \sim 10^3$ in GaAs, here we are using $\Omega/\omega \sim 10 - 10^2$ for the range of Ω considered below. Another difference in comparison with the realistic GaAs dot is that the differences of hf couplings $A_{ij} \equiv A_i - A_j$ (i.e. the differences of Knight shifts of different nuclei) are of the same order of magnitude or larger than the nuclear Zeeman energy differences ω_{ij} , while in GaAs dot with $N > 10^5$ we have $A_{ij} \ll \omega_{ij}$ in the whole range of B fields for which $\delta \ll 1$. Thus, unless we put all the A_i equal one to another, we do not expect to see the ω_{ij} -related oscillation in the SE signal in the heteronuclear system (see Ref. 17 for details on why the $A_{ij} \ll \omega_{ij}$ condition is needed to obtain these oscillations). The existence of this oscillation has been confirmed by recent experiments,²⁶ and here we focus on other aspects of SE decay dynamics.

III. RESULTS FOR SPIN ECHO

First, let us briefly recount what we expect to see in exact numerics at not-too-low magnetic fields ($\delta \ll 1$) based on previous analytical work on spin echo. There should be a “visibility loss” initial decay of SE signal of amplitude $\sim \delta^2$ occurring at timescale of \sqrt{N}/\mathcal{A} (i.e. of order of $O(N^0)$ in units employed here), and we expect a qualitative difference in the magnitude of SE decay between the homonuclear and heteronuclear bath. The open questions are: what is the timescale τ_R on which

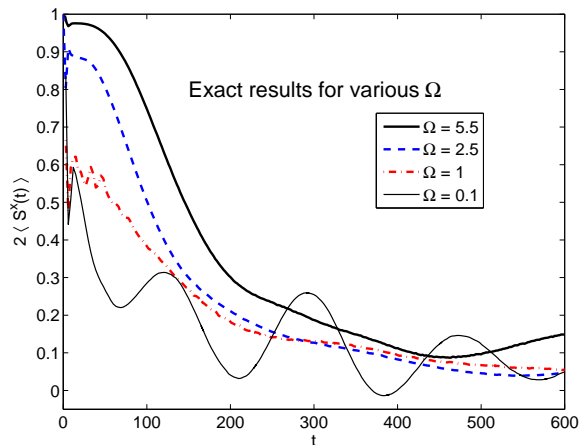


FIG. 1: (Color online) SE decay for $N=20$ nuclei calculated exactly for $\Omega=0.1, 1, 2.5, 5.5$. The hf couplings A_i are given as set 3 in Table I. The energy units are such that $\sum_i A_i^2=1$. The corresponding time units are such that $T_2^* = \sqrt{8}$ (for comparison, $T_2^* \approx 10$ ns in GaAs dots).

the RDT remain quantitatively accurate for $\delta \ll 1$, and what happens at very low B fields at which $\delta \sim 1$ or even $\delta > 1$.

In Figure 1 we are presenting the results of exact calculation for a hetero-nuclear bath with electron Zeeman energies $\Omega \in [0.1, 5.5]$ (corresponding to $\delta \in [0.18, 10]$). As expected, the exact calculation shows a very fast decay having δ^2 magnitude for small δ . In Figure 2 we compare the exact results for $\Omega=2.5$ and 5.5 with the RDT calculations. These calculations were done using the S^z -conditioned interaction from Eq. (2), and also with the S^z -independent two-spin interaction appearing in the 3rd order of the expansion of the effective Hamiltonian,¹⁷ in which the coupling constants are smaller by $\mathcal{A}/N\Omega$ factor. For $\Omega=2.5$ one can see that this 3rd order interaction is not completely irrelevant, signifying the importance of higher-order corrections to the effective Hamiltonian approach. At even lower values of Ω the RDT calculation fails to quantitatively describe the decay: not only it does not capture the very fast initial drop, but also at longer times it predicts a decay much faster than the one given by the exact calculation (these results are not shown, but the beginning of such disagreement between RDT and the exact signal can be seen at $\Omega=2.5$). The oscillatory character of the $\Omega=0.1$ signal will be discussed later in the paper.

On the other hand, at a slightly larger field $\Omega = 5.5$ (when $\delta = 0.18$), the RDT calculation using only the lowest-order hf-mediated interaction is approximating very closely the exact result, and the higher-order corrections are irrelevant. The comparison between RDT and PCA in this case shows how the resummation of all the ring diagrams extends the timescale on which the analytical theory closely matches the exact calculation.

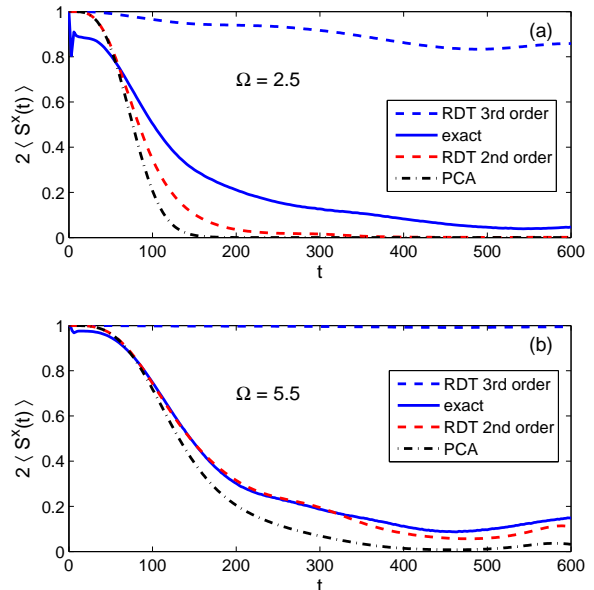


FIG. 2: (Color online) (a) Comparison between the exact (solid line) result for $\Omega = 2.5$, the result obtained using the RDT (red dashed line for 2nd order S^z -conditioned interaction from Eq. (2), blue dashed line for S^z -independent two-spin interaction for the third order effective Hamiltonian), and the result obtained using the Pair Correlation Approximation from Ref. 6 (dot-dashed line). (b) same as (a) only with $\Omega=5.5$.

With $N=20$ it is hard to say with full confidence whether it is the smallness of \mathcal{A}/Ω or $\delta = \mathcal{A}/\sqrt{N}\Omega$ which controls the agreement between the RDT calculation and the exact result. However, it is clearly visible that the onset of long-time agreement between the two calculations correlates with the suppression of the short-time visibility loss, which is known to be controlled by δ . This strongly suggests that it is indeed the smallness of δ that makes the RDT work. Finally, these results are showing that the timescale on which the RDT calculation of SE signal is quantitatively accurate visibly exceeds a value of $\tau_R \approx N/\mathcal{A} \approx \sqrt{20}$, which was conservatively estimated in Ref. 17.

In order to illustrate the degree to which the low-field SE decay is dominated by processes involving nuclei of different species, we have performed the calculations for the homonuclear bath, in which we set all the nuclear Zeeman energies equal to a common value ω . In Fig. 3 we show the exact calculation for $\Omega = 1, 2.5, \text{ and } 5.5$. Now instead of the decay reaching $|W| < 0.1$ in Fig. 1 we see only the initial visibility loss followed by an oscillation with frequency given by the nuclear Zeeman splitting ω .

Within the RDT framework, the lowest-order term in \tilde{H} which contributes to the SE decay in the homonuclear bath is the S^z -independent two-spin interaction from $\tilde{H}^{(3)}$. The decay calculated by RDT with this in-

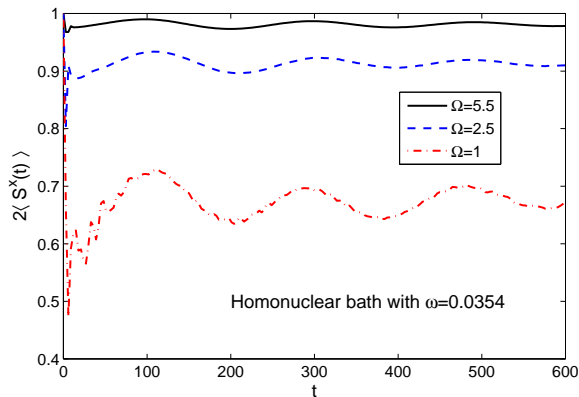


FIG. 3: (Color online) SE decay calculated exactly for $N=20$ with parameters as in Fig. 1, only with all nuclear Zeeman energies set to $\omega=0.0354$.

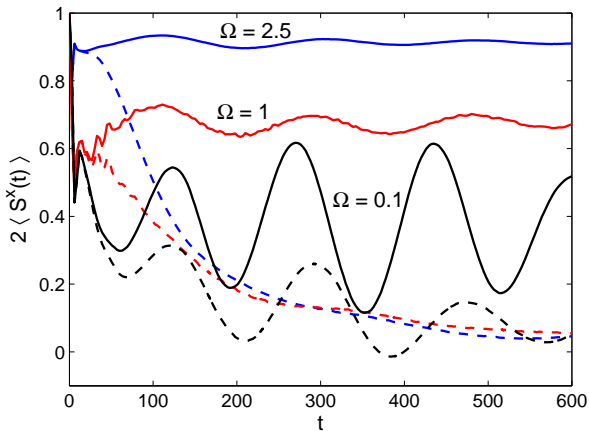


FIG. 4: (Color online) Comparison of the spin echo decay in a heteronuclear bath (dashed lines, parameters the same as in Fig. 1) and a homonuclear bath (solid lines, parameters the same as in Fig. 3) for $\Omega = 2.5, 1, 0.1$ (with the initial decay smallest for the largest Ω).

interaction for $\Omega = 2.5$ in the homonuclear case is very similar to the result shown in Fig. 2a as blue dashed line, and it does not show any oscillation. The same holds for $\Omega = 5.5$ case, where RDT predicts practically no decay in the homonuclear case, while the exact calculation gives the signal oscillating with the nuclear ω frequency around the value of $1 - \delta^2$. Similar oscillations have been found before in numerical simulations of the multi-pulse dynamical decoupling protocols for an electron spin decohered by the nuclear spin bath,²³ where full hyperfine interaction was considered. This shows that this oscillation is a feature following from the full $\mathbf{S} \cdot \mathbf{J}_i$ interaction between the electron and the nuclear spins, and as such cannot be captured by the effective Hamiltonian theory. In this it is similar to the fast initial oscillation with frequency $\sim \Omega$ accompanying the visibility loss. In the next section we discuss a similarity (also noticed in Ref. 23)

between this oscillation and the well-known electron spin echo envelope modulation⁴² (ESEEM).

In Fig. 4 we show the comparison between the exact SE decay in a hetero- and homonuclear bath at very low magnetic fields ($\Omega \leq 2.5$), at which the RDT fails quantitatively. One can see that the qualitative difference between the SE decay in the two cases (homo- vs heteronuclear bath) is also clearly visible for $\Omega = 1$, which is already completely outside the domain of applicability of RDT. In this strongly non-perturbative regime the magnitude of the initial decay ceases to be equal to δ^2 , and instead it is smaller (with $|W| \sim 0.7$ after the initial decay). For the homonuclear bath we then have a small-amplitude oscillation about this value, while the decay in the heteronuclear case is practically complete on the considered timescale. At longer times this decay is very similar to the signal for $\Omega = 2.5$, which also shows the robustness of qualitative predictions of RDT outside the regime of its quantitative applicability: within RDT one obtains B -independent SE decay below a certain value of magnetic field.¹⁷ At even lower values of Ω the situation changes: for $\Omega = 0.1$ the homo- and heteronuclear case signals start to look qualitatively similar. Although the physical picture of hf-mediated interactions is not strictly applicable in this regime, one could qualitatively describe this behavior by saying that the higher order hf-mediated interactions (beyond the second order one, for which the homo- and heteronuclear baths give qualitatively different SE decay) become very strong, and the difference between the two cases disappears. Thus, the oscillatory signal at $\Omega = 0.1$ has a common origin in homo- and hetero-nuclear cases, and the discussion of it is given in the next Section. Let us also note that the $\Omega = 0.1$ SE signal for the heteronuclear case does become negative at some times.

IV. DISCUSSION AND COMPARISON WITH A SIMPLE MODEL

The presence of the oscillation with ω frequency in a *homonuclear* system can be derived using a simplified exactly solvable model,^{8,10,43} in which all the hf couplings A_i are put equal to the same value $A = 1/\sqrt{N}$. The hf Hamiltonian is then given by $A\mathbf{S} \cdot \mathbf{J}$ with $\mathbf{J} \equiv \sum_i \mathbf{J}_i$ being the operator of the total spin of the N nuclei. The calculation of the evolution of the system is most straightforward using the basis of eigenstates of \mathbf{J}^2 and \hat{J}^z . The only pairs of states coupled by the Hamiltonian are then $|\pm, j, m\rangle$ and $|\mp, j, m \pm 1\rangle$, with the first quantum number specifying the central spin state (\pm for electron spin up/down), and we have $\mathbf{J}^2 |j, m\rangle = j(j+1) |j, m\rangle$ and $\hat{J}^z |j, m\rangle = m |j, m\rangle$. Such a simplification of the dynamics of the system does not occur in a heteronuclear case. There we have the full Hamiltonian given by $\hat{H} = \Omega \hat{S}^z + \sum_\alpha \omega_\alpha \hat{J}_\alpha^z + \sum_\alpha A_\alpha \mathbf{S} \cdot \mathbf{J}_\alpha$, and even if we put $A_\alpha = A$ we must retain distinct ω_α . If we then look at the dynamics starting with the initial state, say,

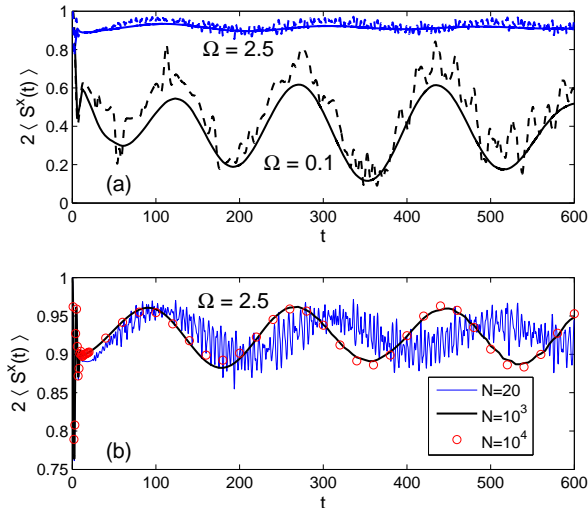


FIG. 5: (Color online) (a) The comparison between the exact results (solid lines) for spin echo in a *homonuclear* system (with the nuclear Zeeman energy $\omega = 0.0354$) for electron spin splitting $\Omega = 2.5, 0.1$ and the results obtained within the model with all the hf couplings A_i being the same (dashed lines). (b) The comparison of such box-wavefunction calculations with different numbers of nuclei N for $\Omega = 2.5$. The fast oscillation is an artifact of small N and the box model, and it disappears with increasing N .

$|+, \{j_\alpha, m_\alpha\}\rangle$ (described by a set of n_J pairs of quantum numbers j_α, m_α for $\alpha = 1 \dots n_J$), we see that the Hamiltonian couples this state to a family of states with central spin down and one m_α increased by 1. Now, unlike in the homonuclear case, these states can also couple to other states which have the electron spin up and m_β (with $\beta \neq \alpha$) decreased by 1. Thus, while in the homonuclear case we only have to solve multiple two-state problems to obtain the system dynamics, in the heteronuclear case we still have to consider Hilbert spaces of dimensions as large as $2 \prod_\alpha (N_\alpha + 1)$ where N_α is the number of nuclei of α species.

The details of this calculation are given in Appendix B, here we focus on the result shown in Fig. 5. In Fig. 5a we present a comparison between the exact calculation with nonuniform A_i (solid lines) and the uniform A_i calculation (dashed lines). The slow oscillation with frequency $\sim \omega$ and the amplitude of the signal is reproduced by the “box wavefunction” calculation. The fast oscillation (with frequency proportional to Ω) visible in the constant A_i calculation is the small N artifact related to artificially regular structure of the Hamiltonian spectrum when all A_i are the same. In Fig. 5b we show the uniform A_i results for $N = 20, 10^3$, and 10^4 . At larger N the fast oscillations disappear, and the shift of the oscillation frequency, while visible, saturates quickly (the results for $N = 10^3$ and 10^4 are practically the same). This allows us to conclude that the presence of the ω -oscillation is

not a small N effect, and that such an oscillation should be present in the SE signal of a central spin interacting with a large homonuclear bath.

For large N the uniform A_i model corresponds to the situation in which a central spin \mathbf{S} interacts with a large spin \mathbf{J} . This leads us to a natural conjecture that the ω -oscillation follows from classical dynamics of the total nuclear spin, i.e. it can be recovered from classical equations of motion for two spins coupled by isotropic Heisenberg coupling and each experiencing a different Zeeman splitting. Since the typical magnitude of the classical nuclear spin \mathbf{J} is proportional to \sqrt{N} , the electron spin precession due to hf coupling is much faster than the nuclear spin precession due to interaction with the electron spin.⁴¹ This leads to averaging out of the electron-induced nuclear precession, which leaves only the nuclear spin precession due to the Zeeman term. One is then looking at a problem of electron spin dynamics due to the magnetic field and also due to the hf coupling with the classical \mathbf{J} vector precessing with frequency ω about the z axis. The appearance of ω frequency in SE signal is then natural. Our preliminary calculations involving averaging of the classical dynamics of coupled \mathbf{S} and \mathbf{J} spins over the ensemble of initial values of \mathbf{J}_0 (without making the adiabatic approximation used above) support this conjecture. This conjecture is also in agreement with the physical picture suggested to explain similar oscillations for multi-pulse dynamical decoupling protocols.²³

Here we can comment on the $\Omega = 0.1$ result from Figs. 1 and 4. At such a low electron spin splitting the SE signal oscillations are present also for the heteronuclear bath. These oscillations are controlled mostly by the 3 nuclear Zeeman frequencies (which we checked by varying ω_α , not shown in the Figures), suggesting that the physical picture described above, albeit with 3 classical nuclear spins, might be a starting point for the description of very low B behavior of the spin echo.

For $\Omega \gg 1$ one can also see a close connection between ω -oscillation of the SE signal and the ESEEM, discussed previously⁴⁰ in the case of a central spin interacting via *anisotropic* hf interaction with the nuclei,⁴⁴ in which case the $\hat{J}^x \hat{S}^z$ coupling was a source of an oscillation of the SE signal. In our case, if we neglect the “visibility loss” effect, the effective Hamiltonian for $\Omega \gg 1$ is given by the sum of $\hat{H}_0 = \Omega \hat{S}^z + \omega \hat{J}^z + A \hat{S}^z \hat{J}^z$ and the hf-mediated interaction from Eq. (2), for which we obtain a perfect recovery of coherence in SE experiment. However, the initial “visibility loss” corresponds to a tilt of the electron spin quantization axis from the original z direction by an angle proportional to δ , and thus the decrease of $\langle \hat{S}^z \rangle$ by a factor $\sim \delta^2$. If we then rotate the coordinate system so that the new z' direction is along the new electron spin quantization axis, we will obtain the terms of $\hat{S}^{z'} \hat{J}^{x'}$ type in \hat{H}_0 defined above, thus arriving at the problem analogous to ESEEM due to anisotropic hf interactions.

The “box wavefunction” approach was used previously to calculate low- B free evolution of S^z component of the central spin,¹⁰ and it was shown to agree with the exact

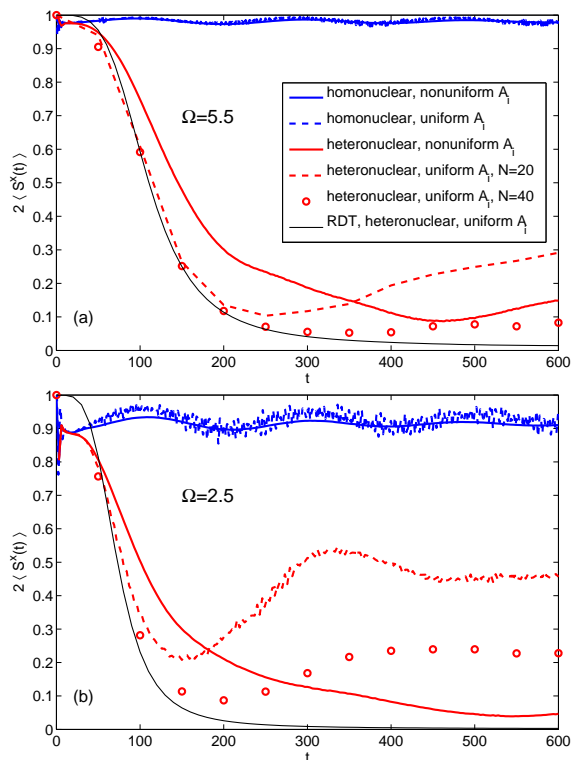


FIG. 6: (Color online) (a) Comparison of the SE signal calculated with non-uniform hf couplings (red and blue solid lines) and with all $A_i = A$ (dashed lines for $N = 20$, circles for $N = 40$) for homonuclear and heteronuclear baths with $N = 20$ and at $\Omega = 5.5$. The thin black solid line is the RDT result for uniform couplings (which is N independent). (b) The same for $\Omega = 2.5$.

solution (for a system with inhomogeneous A_i) on the timescale of $T_2^* \sim \sqrt{N}/\mathcal{A}$. Above we have seen that the box model captures the main features of the SE signal in a homonuclear bath on a much longer timescale, which exceed not only T_2^* but also N/\mathcal{A} .

Interestingly, this agreement between the “box” model and the exact calculation breaks down at shorter timescale for the heteronuclear bath. In Fig. 6 we show the comparison between the nonuniform A_i calculations and the “box” results for homo- and heteronuclear baths (at $\Omega = 2.5, 5.5$ and with $N = 20, 40$ nuclei). The RDT results obtained with the uniform hf couplings are also shown (this calculation gives the SE signal independent of N). For $\Omega = 2.5$ there is an obvious difference in long-time behavior between the “box” calculation and the calculation with nonuniform A_i . The “box” calculation exhibits a saturation of the SE signal at $t \sim 400$ (with the signal staying close to this value for much longer times, not shown in the Figure). However, the amplitude of this saturation decreases with increasing N . While we have $2\langle S^x \rangle_{sat} \approx 0.46$ for $N = 20$, for $N = 40$ we obtain a value of about 0.22, suggesting that these results are affected by finite- N effects. The reason for which these effects are spoiling the agreement between the exact and “box”

calculation only in the heteronuclear case remains to be further elucidated.

At higher Ω , as in Fig. 6a, the finite- N effect is weaker, and with $N = 40$ the RDT and the full-Hamiltonian calculation agree very well for uniform A_i . Both of these signals exhibit a somewhat faster decay than the exact result with nonuniform couplings (which is well reproduced by the RDT calculation with nonuniform A_i , as shown in Fig. 2b). This shows that at $N = 20$ the choice of the specific set of A_i couplings can have a visible impact on the SE signal. This is discussed in more details in Appendix A.

V. CONCLUSIONS

In this paper we have investigated the low magnetic field spin echo (SE) signal of an electron spin interacting via the hyperfine (hf) coupling with the nuclear bath. Intrabath dipolar interactions have been neglected. We have used three theoretical approaches: the exact numerical solution for a relatively small nuclear bath, the analytical theory based on resummation of ring diagrams,^{16,17} and calculations in which uniform hf coupling with all the nuclei was assumed.

The exact numerical calculation strongly suggests that the ring diagram theory (RDT) describes quantitatively the SE decay when the electron Zeeman splitting Ω is much larger than the typical Overhauser field \mathcal{A}/\sqrt{N} (with \mathcal{A} being the total hyperfine interaction and N being the number of nuclei). The timescale τ_R on which RDT describes quantitatively the SE decay well has been shown to visibly exceed N/\mathcal{A} . A qualitative difference between the SE decay due to interaction with the homonuclear and the heteronuclear bath (containing nuclei with distinct Zeeman splittings) is still clearly visible in the numerical calculation for $\Omega \approx \mathcal{A}/\sqrt{N}$ (corresponding to ~ 10 mT in large GaAs dots). Generally, we have found that qualitative and even semi-quantitative predictions of the RDT are robust down to these fields. The saturation of the spin echo decay time at low magnetic fields had been predicted before using the RDT,^{16,17} and our new results lead us to expect that this behavior will be robust down to B fields corresponding to typical Overhauser field, i.e. we predict the SE decay to be practically B -independent between 10 and 100 mT in GaAs quantum dot with $\sim 10^5$ nuclei.

Also, we have found that the SE signal in a homonuclear bath oscillates with the Zeeman frequency of the single present nuclear species. This effect is related to the well-known ESEEM phenomenon, but to our knowledge its presence has not been discussed for the spin echo signal in case of the isotropic hf coupling. This feature might be observed in spin echo experiments on spin qubits in quantum dots based on materials having a single nuclear species, e.g. silicon,^{45,46} carbon nanotubes⁴⁷ or graphene.⁴⁸ In a heteronuclear bath (e.g. in GaAs) we have found that at very low magnetic fields (smaller than

the typical Overhauser field) the spin echo signal exhibits strong oscillations in which the Zeeman frequencies of all the nuclear species are present.

Finally, we have shown that using a simplified model of uniform hf couplings (corresponding to using a box-like electron wavefunction) we can recover certain qualitative features of the SE signal at timescale exceeding both T_2^* and N/A . While the nearly perfect disentanglement of electron spin and nuclear bath by the SE sequence was discussed previously at high magnetic fields,^{6,21} this result of our work suggests that the dynamics of coherence recovery in the SE experiment is quite closely related to classical dynamics of coupled electron and nuclear spins also at much lower magnetic fields. The implications of this observation, and also the analysis of accuracy of analytical theories using the effective hf-mediated interaction for modeling of the narrowed free induction decay, are left for future research.

VI. ACKNOWLEDGEMENTS

This work is supported by LPS-NSA. Work at the Ames Laboratory was supported by the Department of Energy — Basic Energy Sciences under Contract No. DE-AC02-07CH11358. LC also acknowledges support from the Homing programme of the Foundation for Polish Science supported by the EEA Financial Mechanism.

Appendix A: Dependence of the spin echo signal on the choice of hyperfine couplings

In this work we choose the hf couplings A_i randomly from a uniform distribution. The realistic distribution $\rho(A)$ of the A_i couplings is related to the shape of the envelope wavefunction $\Psi(\mathbf{r})$ of the electron:

$$\rho(A) = \frac{1}{\nu_0} \int_V \delta(A - A|\Psi(\mathbf{r})|^2) d^3r, \quad (\text{A1})$$

where V is the total volume, ν_0 is the volume of the unit cell, and the wavefunction normalization is $\int_V |\Psi(\mathbf{r})|^2 d\mathbf{r} = \nu_0$. For the wavefunction being a two-dimensional Gaussian we have $\rho(A) \sim A^{-1} \Theta(A_{\max} - A)$, where $\Theta(x)$ is the Heaviside step function and A_{\max} is the largest hf coupling (for the nucleus located at the center of the wavefunction). $\rho(A)$ for a more realistic electron envelope is given in Ref. 17, and it behaves in qualitatively similar way. The key point is that if we are only concerned about the most strongly coupled nuclei, with A_i not much smaller than A_{\max} (which naturally dominate the decay at short times, and possibly determine most of the decay at low B fields), the approximation of $\rho(A)$ by a constant is reasonable.

The long-time dynamics of the electron spin was predicted to be influenced by the shape, specifically the tails, of the electron wavefunction,^{15,17,18,49–51} and thus the details of the distribution $\rho(A)$ for small A . These features

of $\rho(A)$ are impossible to capture with only $N = 20$ spins. We are, however, not currently concerned about this. The recent experiments²⁶ are showing that the low B field SE decay occurs on timescale $\leq N/A$, on which according to the RDT the wavefunction shape is relatively unimportant. Thus the question of low-field accuracy of the RDT for an uniform distribution of A_i is well motivated.

It is nevertheless prudent to check how our results depend on the randomly chosen set of A_i . The reasonable expectation is that for large N the choice should not matter. This is *not* the case with $N \leq 10$, with which both the exact and RDT results are showing very diverse behavior beyond the short time limit (i.e. $t < 100$ for $N = 10$). Unsurprisingly, for such small N the agreement between the two calculations is also present only for these short times. For $N = 20$ the situation already becomes much closer to our expectations. In Fig. 7 we present the RDT results for 20 random choices of the set of A_i couplings at $\Omega = 5.5$. One can see that the typical decay signal is clearly visible. However, there are still sets of hf couplings which give SE signals visibly differing from the typical behavior. The two most extreme cases are drawn with dashed lines in Fig. 7. The set of A_i used in previous calculations corresponds to the dot-dashed line. This signal is quite close to the typical one, although it does possess characteristic features. These features closely correspond to the ones of the exact signal shown before in Fig. 2b, showing that at $\Omega = 5.5$ the RDT calculation is very close to the exact one for “typical” choice of A_i .

In Fig. 8 we present the comparison between the RDT and exact results for two sets of A_i corresponding to most atypical results from Fig. 7. The values of hf couplings used in these calculations are given in Table I, together with the set of A_i used in most of the other figures in the paper. For the signal showing very weak decay (set 1) we find quite a good agreement. For the signal exhibiting a sharp peak (set 2) the agreement could be considered quantitative.

We have checked that the special behavior in case of set 2 is due to presence of a large number of very small couplings in this set. In fact, one can remove more than 10 smallest A_i from this set without visibly affecting the results, while the decay becomes completely different (and much weaker) when one of the large couplings, A_{19} , is removed.

In the case of set 1, the agreement is almost quantitative (only the slow oscillation seems to be the artifact of RDT) As for the reason for the exceptionally weak decay, it is possible that after removing the A_i couplings which are too small to visibly affect the signal, the remaining couplings, especially the ones for different species of nuclei (since hetero-nuclear interactions are crucial for SE decay) are *too uniform*. We note that as shown in Fig. 6, the decay for $N = 20$ with *uniform* couplings saturates at about a half of initial value of the signal. This saturation effect becomes weaker when N is increased.

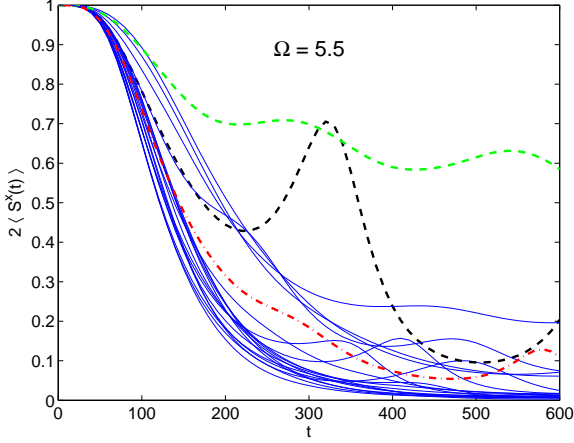


FIG. 7: (Color online) RDT calculation of the SE signal at $\Omega = 5.5$ performed for 20 different sets of hf couplings A_i (drawn at random from a uniform distribution, with $\sum_i A_i^2 = 1$ normalization). The signal for the set used in previous figures is given by the red dot-dashed line. Two of the most “atypical” signals are drawn with dashed lines.

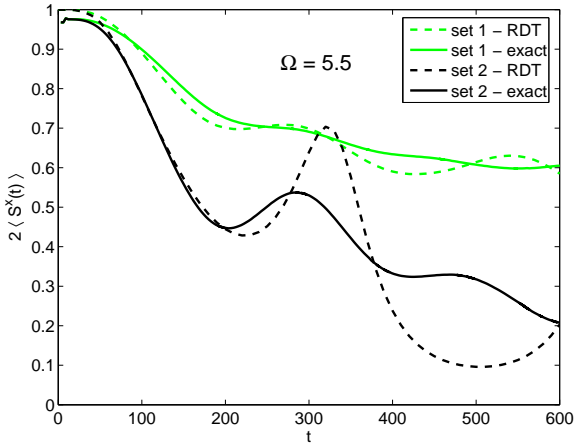


FIG. 8: (Color online) The comparison the the RDT calculation (dashed lines) and the exact calculation (solid lines) for the two sets of hf couplings which give atypical SE signals (shown in Fig. 7 by dashed lines)

It is also interesting to consider how the choice of the hf coupling parameters affects the SE signal in the experimentally relevant limit of very large N . We consider the SE signal $S(t)$, given by

$$S(2\tau) = \text{Tr}[\hat{S}_x e^{-i\hat{H}\tau} \hat{\sigma}_x e^{-i\hat{H}\tau} \hat{S}_x e^{i\hat{H}\tau} \hat{\sigma}_x e^{i\hat{H}\tau}], \quad (\text{A2})$$

which is just another way to write Eq. (4). To access the limit of large N , we can use the Levy’s lemma.^{52,53} It states that for a function $f(\vec{x})$ defined on a $(N - 1)$ -dimensional hypersphere $\vec{x} \in S^{N-1}$, and satisfying the 1-Lipshitz condition, the value of the function at a randomly chosen point is close to the average value of this

| spin number i | A_i (set 1) | A_i (set 2) | A_i (set 3) |
|-----------------|---------------|---------------|---------------|
| 1 | 0.1236 | 0.2681 | 0.2167 |
| 2 | 0.3984 | 0.3087 | 0.1746 |
| 3 | 0.0376 | 0.1651 | 0.1033 |
| 4 | 0.1999 | 0.2836 | 0.2253 |
| 5 | 0.0017 | 0.3709 | 0.2974 |
| 6 | 0.1120 | 0.0088 | 0.1769 |
| 7 | 0.0007 | 0.0383 | 0.2123 |
| 8 | 0.0960 | 0.4457 | 0.3171 |
| 9 | 0.0723 | 0.2978 | 0.3479 |
| 10 | 0.1360 | 0.1057 | 0.1659 |
| 11 | 0.0887 | 0.1845 | 0.1655 |
| 12 | 0.0704 | 0.0558 | 0.2818 |
| 13 | 0.3039 | 0.1227 | 0.0928 |
| 14 | 0.4572 | 0.1179 | 0.1386 |
| 15 | 0.4767 | 0.1516 | 0.1520 |
| 16 | 0.1122 | 0.0696 | 0.1225 |
| 17 | 0.2449 | 0.1591 | 0.0926 |
| 18 | 0.1908 | 0.0556 | 0.1416 |
| 19 | 0.2658 | 0.4042 | 0.3951 |
| 20 | 0.1344 | 0.0431 | 0.3001 |

TABLE I: Three sets of hf couplings A_i : sets 1 and 2 correspond, respectively, to the most weakly decaying signal and to the signal with prominent peak at $t \approx 350$ shown in Fig. 7, while set 3 has been used in all the previous figures. The values of ω_i nuclear Zeeman energies are: $\omega_i = 0.02526$ for $i \leq 10$, $\omega_i = 0.0354$ for $i \in [11, 16]$ and $\omega_i = 0.045$ for $i \in [17, 20]$.

function $\langle f \rangle$ with very high probability:

$$\text{Prob}[|f(\vec{x}) - \langle f \rangle| > \epsilon] \leq \exp(-CN\epsilon^2/L^2) \quad (\text{A3})$$

where $L = \sup|\nabla f|$ is the Lipshtiz constant. We use the vector $(A_1, A_2, \dots, A_k, \dots, A_N)$ of the coupling constants, with normalization $\sum_k A_k^2 = 1$, as a point \vec{x} on a N -dimensional hypersphere, and the SE signal $S(t)$ as a function $f(\vec{x})$. To evaluate L , we have to find the derivatives of $\partial S(t)/\partial A_k$, taking into account that the only quantity dependent on A_k in Eq. (A2) is the Hamiltonian \hat{H} . Thus, we need to substitute the equality

$$\begin{aligned} \frac{\partial}{\partial A_k} e^{-i\hat{H}\tau} &= e^{-i\hat{H}\tau} \int_0^\tau ds e^{i\hat{H}s} \frac{\partial \hat{H}}{\partial A_k} e^{-i\hat{H}s} \quad (\text{A4}) \\ &= e^{-i\hat{H}\tau} \int_0^\tau ds (\mathbf{S}\mathbf{J}_k)(s) \end{aligned}$$

(and its Hermitian-conjugated version) into four places in Eq. (A2). In the Equation above $(\mathbf{S}\mathbf{J}_k)(s) = e^{i\hat{H}s} (\mathbf{S}\mathbf{J}_k) e^{-i\hat{H}s}$. Furthermore, we should take into account that the trace of a matrix product $\text{Tr}[\hat{A}^\dagger \hat{B}]$ has all properties of the scalar product, so that

$$|\text{Tr}[\hat{A}^\dagger \hat{B}]| \leq \sqrt{\text{Tr}[\hat{A}^\dagger \hat{A}] \text{Tr}[\hat{B}^\dagger \hat{B}]} = \|\hat{A}\| \|\hat{B}\|, \quad (\text{A5})$$

where $\|A\| = \sqrt{\text{Tr}[A^\dagger A]}$. As a result, we obtain

$$\left| \frac{\partial S(t)}{\partial A_k} \right| \leq 4 \|\hat{S}_x^2\| \int_0^\tau ds \|(\mathbf{S}\mathbf{J}_k)(s)\| = \sqrt{2} \int_0^\tau ds \|(\mathbf{S}\mathbf{J}_k)(s)\|. \quad (\text{A6})$$

Therefore,

$$\left| \frac{\partial S(t)}{\partial A_k} \right| \leq C_1 t \quad (\text{A7})$$

with some constant C_1 independent of N , and for the Lipschitz constant we obtain

$$L \leq C_1 t \sqrt{N}. \quad (\text{A8})$$

Thus, for $t \sim 1$ (in our dimensionless units, where $\sum_k A_k^2 = 1$), the specific choice of the hf coupling parameters does not matter.

However, it is obvious that our rigorous estimate Eq. (A6), which is based on straightforward use of the Cauchy inequality, is too crude. Heuristically, we expect that the correlation between the central spin and a single bath spin, which we crudely estimated from above as $O(1)$, is actually of order of $O(1/N)$. Then, the range of times where the choice of the hf parameters does not matter, is extended to $t \sim N$.

Appendix B: Spin echo in a model with uniform hf couplings

We rewrite Eq. (4) using the basis of $|\pm, j, m\rangle$ states (with electron states $|\pm x\rangle = (|+\rangle \pm |-\rangle)/\sqrt{2}$) and with $\tau \equiv t/2$

$$\langle \hat{S}^x(t) \rangle = \frac{1}{2^N} \sum_j \sum_{m=-j}^j D_j \langle +x, j, m | e^{i\hat{H}t\tau} \hat{\sigma}_x e^{i\hat{H}\tau} \frac{\hat{\sigma}_x}{2} e^{-i\hat{H}\tau} \hat{\sigma}_x e^{-i\hat{H}\tau} | +x, j, m \rangle \quad (\text{B1})$$

where the sum over j is from 0 to $N/2$ ($1/2$ to $N/2$) for even (odd) number of nuclei N , and the degeneracies of states with given j are given by⁴³

$$D_j = \frac{N!}{(N/2 - j)!(N/2 + j)!} \frac{2j + 1}{N/2 + j + 1}. \quad (\text{B2})$$

As discussed in Sec. IV, the Hamiltonian couples only pairs of $|\pm, j, m\rangle$ states:

$$e^{-i\hat{H}\tau} |+, j, m\rangle = a_{jm} |+, j, m\rangle + b_{jm} |-, j, m + 1\rangle \quad (\text{B3})$$

$$e^{-i\hat{H}\tau} |-, j, m\rangle = c_{jm} |-, j, m\rangle + d_{jm} |+, j, m - 1\rangle \quad (\text{B4})$$

and the coefficients a_{jm} and b_{jm} are given by

$$a_{jm} = e^{-iE_m^+ \tau} \left(\cos \frac{N_{jm}^+ \tau}{2} - i \frac{Z_m^+}{N_{jm}^+} \sin \frac{N_{jm}^+ \tau}{2} \right) \quad (\text{B5})$$

$$b_{jm} = -i e^{-iE_m^+ \tau} \frac{X_{jm}^+}{N_{jm}^+} \sin \frac{N_{jm}^+ \tau}{2}, \quad (\text{B6})$$

and c_{jm} and d_{jm} are given by analogous expressions with superscripts $+$ replaced by $-$. E_m^\pm , X_m^\pm , Z_m^\pm and N_m^\pm are given by

$$E_m^\pm = [(2m \pm 1)\omega - A/2]/2, \quad (\text{B7})$$

$$X_{jm}^\pm = A \sqrt{j(j+1) - m(m \pm 1)}, \quad (\text{B8})$$

$$Z_m^\pm = \pm[\Omega - \omega + A(m \pm 1/2)], \quad (\text{B9})$$

$$N_{jm}^\pm = \sqrt{(X_{jm}^\pm)^2 + (Z_m^\pm)^2}. \quad (\text{B10})$$

Plugging these into Eq. (B1) and into an analogous expression for $\langle \hat{S}^y(t) \rangle$ (in which the middle $\hat{\sigma}_x$ operator is replaced by $\hat{\sigma}_y$) we arrive at the formula for the decoherence function

$$W^{SE}(t) = \sum_{j=0}^{N/2} \sum_{m=-j}^j \frac{D_j}{2^N} \left(|a_{jm} c_{jm}|^2 + a_{jm} c_{jm}^* a_{j,m-1} d_{jm} |^2 + a_{j,m+1} c_{jm}^* |b_{jm}|^2 \right). \quad (\text{B11})$$

In the case of heteronuclear bath with N_j nuclear species one has to introduce N_j sets of basis states $|j_\alpha, m_\alpha\rangle$ in Eq. (B1). The Hamiltonian is then coupling the whole subspaces of fixed j_α , and one has to consider Hamiltonian matrices of dimension $2 \prod_\alpha (2j_\alpha + 1)$ and evaluate the evolution operators numerically.

* Electronic address: lcyw@ifpan.edu.pl

¹ R. Hanson, L. P. Kouwenhoven, J. R. Petta, S. Tarucha, and L. M. K. Vandersypen, Rev. Mod. Phys. **79**, 1217 (2007).

² W. A. Coish and J. Baugh, Phys. Status Solidi B **246**, 2203 (2009).

³ R. de Sousa and S. Das Sarma, Phys. Rev. B **68**, 115322 (2003).

⁴ W. M. Witzel, R. de Sousa, and S. Das Sarma, Phys. Rev.

B **72**, 161306(R) (2005).

⁵ W. M. Witzel and S. Das Sarma, Phys. Rev. B **74**, 035322 (2006).

⁶ W. Yao, R.-B. Liu, and L. J. Sham, Phys. Rev. B **74**, 195301 (2006).

⁷ W. M. Witzel and S. Das Sarma, Phys. Rev. B **77**, 165319 (2008).

⁸ A. Khaetskii, D. Loss, and L. Glazman, Phys. Rev. B **67**, 195329 (2003).

- ⁹ W. A. Coish and D. Loss, Phys. Rev. B **70**, 195340 (2004).
- ¹⁰ W. Zhang, V. V. Dobrovitski, K. A. Al-Hassanieh, E. Dagotto, and B. N. Harmon, Phys. Rev. B **74**, 205313 (2006).
- ¹¹ R.-B. Liu, W. Yao, and L. J. Sham, New J. Phys. **9**, 226 (2007).
- ¹² S. K. Saikin, W. Yao, and L. J. Sham, Phys. Rev. B **75**, 125314 (2007).
- ¹³ C. Deng and X. Hu, Phys. Rev. B **73**, 241303(R) (2006).
- ¹⁴ C. Deng and X. Hu, Phys. Rev. B **78**, 245301 (2008).
- ¹⁵ W. A. Coish, J. Fischer, and D. Loss, Phys. Rev. B **77**, 125329 (2008).
- ¹⁶ L. Cywiński, W. M. Witzel, and S. Das Sarma, Phys. Rev. Lett. **102**, 057601 (2009).
- ¹⁷ L. Cywiński, W. M. Witzel, and S. Das Sarma, Phys. Rev. B **79**, 245314 (2009).
- ¹⁸ W. A. Coish, J. Fischer, and D. Loss, Phys. Rev. B **81**, 165315 (2010).
- ¹⁹ J. Schliemann, A. Khaetskii, and D. Loss, J. Phys.:Condens. Matter **15**, R1809 (2003).
- ²⁰ V. V. Dobrovitski and H. A. De Raedt, Phys. Rev. E **67**, 056702 (2003).
- ²¹ N. Shenvi, R. de Sousa, and K. B. Whaley, Phys. Rev. B **71**, 224411 (2005).
- ²² W. Zhang, N. Konstantinidis, K. A. Al-Hassanieh, and V. V. Dobrovitski, J. Phys.:Condens. Matter **19**, 083202 (2007).
- ²³ W. Zhang, N. P. Konstantinidis, V. V. Dobrovitski, B. N. Harmon, L. F. Santos, and L. Viola, Phys. Rev. B **77**, 125336 (2008).
- ²⁴ J. R. Petta, A. C. Johnson, J. M. Taylor, E. A. Laird, A. Yacoby, M. D. Lukin, C. M. Marcus, M. P. Hanson, and A. C. Gossard, Science **309**, 2180 (2005).
- ²⁵ F. H. L. Koppens, K. C. Nowack, and L. M. K. Vander-sypen, Phys. Rev. Lett. **100**, 236802 (2008).
- ²⁶ H. Bluhm, S. Foletti, I. Neder, M. Rudner, D. Mahalu, V. Umansky, and A. Yacoby, arXiv:1005.2995 (2010).
- ²⁷ A. Greilich, S. E. Economou, S. Spatzek, D. R. Yakovlev, D. Reuter, A. D. Wieck, T. L. Reinecke, and M. Bayer, Nat. Phys. **5**, 262 (2009).
- ²⁸ D. Press, K. De Greve, P. L. McMahon, T. D. Ladd, B. Friess, C. Schneider, M. Kamp, S. Höfling, A. Forchel, and Y. Yamamoto, Nat. Photon. **4**, 367 (2010).
- ²⁹ S. M. Clark, Kai-Mei C. Fu, Q. Zhang, T. D. Ladd, C. Stanley, and Y. Yamamoto, Phys. Rev. Lett. **102**, 247601 (2009).
- ³⁰ D. Klauser, W. A. Coish, and D. Loss, Phys. Rev. B **73**, 205302 (2006).
- ³¹ A. Greilich, D. R. Yakovlev, A. Shabaev, A. L. Efros, I. A. Yugova, R. Oulton, V. Stavarache, D. Reuter, A. Wieck, and M. Bayer, Science **313**, 341 (2006).
- ³² L. Viola, J. Mod. Opt. **51**, 2357 (2004).
- ³³ W. Yao, R.-B. Liu, and L. J. Sham, Phys. Rev. Lett. **98**, 077602 (2007).
- ³⁴ W. M. Witzel and S. Das Sarma, Phys. Rev. Lett. **98**, 077601 (2007).
- ³⁵ W. M. Witzel and S. Das Sarma, Phys. Rev. B **76**, 241303(R) (2007).
- ³⁶ A. Grishin, I. V. Yurkevich, and I. V. Lerner, Phys. Rev. B **72**, 060509(R) (2005).
- ³⁷ W. Yang and R.-B. Liu, Phys. Rev. B **78**, 085315 (2008).
- ³⁸ R. M. Lutchyn, L. Cywiński, C. P. Nave, and S. Das Sarma, Phys. Rev. B **78**, 024508 (2008).
- ³⁹ A. M. Tyryshkin, J. J. L. Morton, S. C. Benjamin, A. Ardavan, G. A. D. Briggs, J. W. Ager, and S. A. Lyon, J. Phys. Condens. Matter **18**, S783 (2006).
- ⁴⁰ W. M. Witzel, X. Hu, and S. Das Sarma, Phys. Rev. B **76**, 035212 (2007).
- ⁴¹ I. A. Merkulov, A. L. Efros, and M. Rosen, Phys. Rev. B **65**, 205309 (2002).
- ⁴² W. B. Mims, Phys. Rev. B **5**, 2409 (1972).
- ⁴³ A. Melikidze, V. V. Dobrovitski, H. A. De Raedt, M. I. Katsnelson, and B. N. Harmon, Phys. Rev. B **70**, 014435 (2004).
- ⁴⁴ S. Saikin and L. Fedichkin, Phys. Rev. B **67**, 161302(R) (2003).
- ⁴⁵ N. Shaji, C. B. Simmons, M. Thalakulam, L. J. Klein, H. Qin, H. Luo, D. E. Savage, M. G. Lagally, A. J. Rimberg, R. Joynt, et al., Nat. Phys. **4**, 540 (2008).
- ⁴⁶ E. P. Nordberg, G. A. T. Eyck, H. L. Stalford, R. P. Muller, R. W. Young, K. Eng, L. A. Tracy, K. D. Childs, J. R. Wendt, R. K. Grubbs, et al., Phys. Rev. B **80**, 115331 (2009).
- ⁴⁷ H. O. H. Churchill, F. Kueemeth, J. W. Harlow, A. J. Bestwick, E. I. Rashba, K. Flensberg, C. H. Stwertka, T. Taychatanapat, S. K. Watson, and C. M. Marcus, Phys. Rev. Lett. **102**, 166802 (2009).
- ⁴⁸ J. Fischer, B. Trauzettel, and D. Loss, Phys. Rev. B **80**, 155401 (2009).
- ⁴⁹ S. I. Erlingsson and Y. V. Nazarov, Phys. Rev. B **70**, 205327 (2004).
- ⁵⁰ K. A. Al-Hassanieh, V. V. Dobrovitski, E. Dagotto, and B. N. Harmon, Phys. Rev. Lett. **97**, 037204 (2006).
- ⁵¹ G. Chen, D. L. Bergman, and L. Balents, Phys. Rev. B **76**, 045312 (2007).
- ⁵² J. Matousek, *Lectures on Discrete Geometry* (Springer Verlag, Berlin, New York, 2002).
- ⁵³ S. Popescu, A.J. Short, and A. Winter, Nat. Phys. **2**, 754 (2006); arXiv:quant-ph/0511225 (2005).